

Article

Robust Statistical Approaches for RSS-Based Floor Detection in Indoor Localization

Alireza Razavi*, Mikko Valkama, and Simona Lohan

Department of Electronics and Communications Engineering, Tampere University of Technology, Tampere, Finland.

e-mail: arazavi@ieee.org, mikko.e.valkama@tut.fi, elena-simona.lohan@tut.fi

* Correspondence: arazavi@ieee.org; Tel.: +358404192021

Version May 17, 2016 submitted to Sensors; Typeset by L^AT_EX using class file mdpi.cls

Abstract: Floor detection for indoor 3D localization of mobile devices is nowadays an important challenge in wireless world. Many approaches currently exist, but usually the robustness of such approach is not addressed or investigated. The goal of this paper is to show how to robustify the floor estimation, when probabilistic approaches with a low number of parameters are employed. Indeed, such approach would allow a building-independent estimation and a lower computing power at the mobile side. Four robustified algorithms are to be presented: robust weighted centroid localization method, robust linear trilateration method, robust nonlinear trilateration method, and robust deconvolution method. The proposed approaches use the received signal strengths (RSS) measured by the Mobile Station (MS) from various heard WiFi access points (APs) and provide an estimate of the vertical position of the MS which can be used for floor detection. We will show that robustification can indeed increase the performance of the RSS-based floor detection algorithms.

Keywords: Indoor localization, floor detection, RSS-based localization, robust regression, weighted centroid localization, trilateration.

1. Introduction

Indoor localization is becoming more and more important in today's wireless world. Being able to achieve accurate ubiquitous localization on hand-held battery operating mobile devices in both indoor and outdoor environments would open the window to many new Location Based Services (LBS). Despite the fact that outdoor global localization solutions exist nowadays with the help of Global Navigation Satellite Systems (GNSS), global solutions for indoor localization are still hard to find. Fingerprinting (FP) approaches can solve the indoor localization problem locally [1], but such solutions are expensive and rather computationally expensive to be used on a global scale (e.g. worldwide). In the fingerprinting-based methods, the location service providers construct a fingerprint database, transfer this database to the MS, and the MS then computes its location based on similar fingerprints. The fingerprint databases are typically very large since they do contain RSSs coming from various APs and in many points or coordinates within a building. Thus, if a global localization solution would use a fingerprinting approach, the fingerprint database transferred from the server to the MS would include the fingerprints from all essential buildings in the town (or the location area) where the mobile is situated. For example, assuming that we hear an average of 30 APs in each location point inside a building, that we take measurements from an average of 600 location points per building, that there are 25 important buildings (malls, shopping centers, hospitals, airports, ...) in the location area where the mobile was identified by the network, then a total of 495000 parameters would need to be stored in the database pertaining to that town and transferred to the mobile. The parameters are the fingerprints, namely the (x, y, z) coordinates and the measured

RSS values per coordinate. In addition, if these parameters are saved with a 32-bit accuracy, the database size of such a server provider for the particular town of our example would be around 15.86 Mbits. Assuming that many users are downloading simultaneously this amount of positioning data from the network, the network would soon become very crowded and the data capacity for wireless communications would be tremendously decreased in order to support the positioning requests. This easily could create a bottleneck on the server side, thus it is very important to find statistical methods to use instead of fingerprinting, in order to decrease the amount of parameters to be sent to the mobile, and that the data usage for positioning purpose.

There are two alternative ways to address these problem: one is to compute the user's location entirely at the server side, and the second one is to use a probabilistic approach, where what we transfer to the mobile is a smaller number of parameters, extracted in a statistical way from the database. The first solution, which is entirely network-based, suffers from several drawback: it offers the user location with some delays (due to the propagation delays between the MS and the network server), and with reduced accuracy (due to the fact that the MS might move between the moment when it sent its location request to the server and until the location computed by the server reaches it). Additionally, since the user location needs to be provided on a continuous basis and for users from different towns, if a significant number of users send their location requests to the location server, then the amount of processing required at the server side also becomes fast unfeasible.

The second approach which alleviates all these problems (the need for transferring huge databases with fingerprints and the problem of dealing with huge amount of data at server side when the positioning is purely network based) is the approach addressed in this paper. Here, the positioning and floor estimation is done entirely by the mobile device, and the location server transfers only a small amount of data to the MS. In the probabilistic approaches, instead of transferring the fingerprints database, we only transfer few parameters per each AP in a building (5 parameters per AP, as in path loss model (4)). Taking the previous example and assuming an average of 150 APs per building, the server would need to transfer to the MS only 18750 parameters, or 0.6 Mbits, which would take at most 12 seconds with the average speed of 50 kbps. This time already becomes comparable with the cold start-up times in modern GPS receivers. Therefore, the mobile-computing localization algorithms developed based on this approach are highly suitable for the mobile devices of tomorrow which support localization and navigation features. The algorithms developed in this paper lie within this approach.

Due to the unavailability of true channel model as well as the distribution of noise/modelling errors, most of the probabilistic approaches, whether explicitly or implicitly, employ the standard least-squares (LS) method, which is optimum in the maximum-likelihood sense under the Gaussianity assumption. This assumption may impose significant errors especially when the noise/modeling error expose outliers or have tails heavier than Gaussian distribution.

In this paper, we employ M-estimators as a means for robustifying the probabilistic positioning methods, when the model of noise/modelling errors deviates from Gaussianity. The term *M*-estimation is used because this class of estimators can be regarded as a generalization of Maximum-likelihood estimation [2]. We show how M-estimates can be deployed in four existing positioning methods, namely Weighted Centroid Localization (WCL) [3], linear and nonlinear trilateration [4], and deconvolution-based method [5]. The comparison between the performance of ordinary and robustified version for each method is studied using some numerical result which verifies that the M-estimates can provide higher degree of robustness for these methods.

The potential applications are when a user wants to use his/her smart phone to localize himself/herself inside a multi-floor building, e.g. a shopping mall, that the user may visit for the first time, and possibly guide him/her to a certain or favorite place, e.g. the closest shoe store, inside the building. The application that the user uses on the smart phone can have a complete map of the shopping mall including the 3-dimensional coordinates of all the stores and places inside the building, but to be able to guide him/her to the favorite place it should be able to first localize itself. We would

Table 1. Most important positioning-related notations used in this paper.

Quantity	Notation
Number of fingerprints	N_{FP}
Number of Access Points	N_{AP}
online 3-D coordinates of MS	$\mathbf{c} \triangleq (x, y, z)$
3-D coordinates of i -th access point	$\mathbf{c}_i \triangleq (x_i, y_i, z_i)$
3-D coordinates of i -th fingerprint	$\underline{\mathbf{c}}_i \triangleq (\underline{x}_i, \underline{y}_i, \underline{z}_i)$
The RSS of ap -th AP at n -th fingerprint	$P_{n,ap}$
The $N_{AP} \times 1$ measurement vector at n -th fingerprint	$\mathbf{m}_n \triangleq [P_{n,1}, P_{n,2}, \dots, P_{n,N_{AP}}]^T$
The RSS of ap -th AP received by MS in online phase	p_{ap}
The $N_{AP} \times 1$ measurement vector in online phase	$\mathbf{m}_{MS} \triangleq [p_1, p_2, \dots, p_{N_{AP}}]^T$

mention here that the focus of this work is on the z -axis localization rather than the three-dimensional (x, y, z) localization. Recently, there has been an increasing interest in estimating the z coordinates due to the fact that finding the correct floor is more important than (x, y) coordinates as few meters error in estimation of z -coordinates may lead the mobile user to a wrong floor in positioning [6–8].

The novelty of our paper is two folds: first, we present four innovative robustification methods for mobile-based floor detection in wireless positioning, and second, we validate our algorithms through measured and simulated data and we show their feasibility in realistic multi-floor scenarios. We point out that the goal of this paper is not to compare different RSS-based localization algorithms (or their robustified counterparts) but rather to show that the robustification can improve the performance of each method.

The organization of this paper is as follows: in Section 2 we describe the system model and briefly explain two celebrated methods of indoor localization, namely fingerprinting approach and path-loss approach. The theoretical contribution of the paper is introduced in Section 3 where after describing the M -estimates of regression we will exploit it to robustify four existing indoor localization approaches. Section 4 is devoted to the performance analysis of the proposed robust localization approaches based on numerical real-life measurements and a simulation experiments is provided in Section 5. Finally, we conclude the paper in Section 6.

Notations: Throughout this paper matrices are denoted by capital boldface letters and vectors and tuples are denoted by small boldface letters. $=$ denotes the equality and \triangleq denotes the definition. Besides, Table 1 summarizes the most important notations used for denoting quantities used in positioning in this paper.

2. System Model and Background on Indoor Localization Methods

Consider a localization system equipped with N_{AP} positioning signals (e.g., RSS values received from APs). During the offline phase, the positioning signals are collected in $N_{AP} \times 1$ measurements vectors $\mathbf{m}_i \triangleq [P_{i,1}, P_{i,2}, \dots, P_{i,N_{AP}}]^T$, $i = 1, \dots, N_{FP}$, where N_{FP} is the number of fingerprints collected in the building and $P_{n,ap}$ is the RSS received from access point ap at n -th collected fingerprint. The corresponding known 3-D location of \mathbf{m}_i is denoted by $\underline{\mathbf{c}}_i \triangleq (\underline{x}_i, \underline{y}_i, \underline{z}_i)$, $i = 1, \dots, N_{FP}$. We will use the stored data, $\mathcal{D} \triangleq \{\mathbf{m}_i, \underline{\mathbf{c}}_i, i = 1, \dots, N_{FP}\}$, for indoor localization. In the following we briefly explain two of the famous methods, a nonparametric method and a parametric method, for indoor localization based on the stored data. Then in Section 3 we will introduce some robust methods for indoor localization.

2.1. Fingerprinting Localization

In fingerprinting approach [9–11], the fingerprints $\{\mathbf{m}_i, \underline{\mathbf{c}}_i, i = 1, \dots, N_{FP}\}$, are stored and directly used for localization purposes.

Assume that a Mobile Station (MS) located at unknown coordinates $\mathbf{c} = (x, y, z)$ observes a positioning vector $\mathbf{m}_{\text{MS}} \triangleq [p_1, p_2, \dots, p_{N_{\text{AP}}}]^T$, where p_{ap} , $ap = 1, \dots, N_{\text{AP}}$, is the RSS received from ap -th AP during the online phase. The basic 1-Nearest Neighbor (1-NN) fingerprinting (FP) approach estimates the location of the MS as

$$\hat{\mathbf{c}}_{\text{FP}} = \mathbf{c}_j, \quad (1)$$

where

$$j = \arg \min_{i \in \{1, \dots, N_{\text{FP}}\}} d(\mathbf{m}_{\text{MS}}, \mathbf{m}_i), \quad (2)$$

and $d(\cdot, \cdot)$ is a dissimilarity measure which is determined based on our assumption for noise. For instance if we assume that the noise which deviates the \mathbf{m}_{MS} from \mathbf{m}_i is i.i.d white Gaussian, then $d(\mathbf{m}_{\text{MS}}, \mathbf{m}_i)$ is simply the squared Euclidean distance between \mathbf{m}_{MS} and \mathbf{m}_i , i.e.,

$$d(\mathbf{m}_{\text{MS}}, \mathbf{m}_i) = \|\mathbf{m}_{\text{MS}} - \mathbf{m}_i\|_2^2. \quad (3)$$

In general, fingerprint-based localization approach is a *pattern matching* approach [9–11], rooted in pattern recognition [12], which tries to match the pattern \mathbf{m}_{MS} observed by MS to the examples $\{\mathbf{m}_i\}_{i=1}^{N_{\text{FP}}}$ collected in the training data set and chooses the location of the less dissimilar example (fingerprint) as the location of MS. In this regard, each element of measurements vector \mathbf{m}_i is a *feature* of the location \mathbf{c}_i . On the other hand, any measured signal which depends *only on the measurement location* (regardless of noise, shadowing and other uncertainties), can be regarded as a *feature* of that location and used for localization using fingerprinting scheme.

The main problem with the fingerprinting approach is the huge amount of data which must be stored by servers and transmitted to the MS to localize itself when N_{FP} is a large number. The situation becomes even more severe when the fingerprints are being collected all over the time. If we want to use fingerprinting methods for localizing the mobile device, it can only be done on the server side. Because of the limited processing capability and power supply on most of the mobile devices, they are not capable of storing and processing of that huge amount of data [13] and furthermore transmitting such amount of fingerprinting data from server to the mobile device takes a lot of time, which makes the localization by mobile devices impractical.

2.2. Path-loss approach for indoor localization

To cope with this problem, a well-known alternative is to use the so called model-based (or parametric) approaches for indoor localization. In model-based approaches we use a parametric model for finding the MS location. The parameters of the model are then estimated based on the training data (fingerprinting data) and the MS only stores these parameters and use them for localization by applying it to the online received positioning vector. In the following we briefly describe a parametric approach for indoor localization based on path-loss model.

Any RSS-based localization and floor detection method includes two stages: a training stage and an estimation stage. In the training stage, done either in a dedicated/manual mode or in a crowdsourcing mode, the data is collected building by building and the fingerprinting database \mathcal{D} is stored on a server database. In the path-loss approach of doing the localization, which is one of the main parametric approaches for localization, the target is to extract a sub-set \mathcal{S} of relevant information starting from \mathcal{D} . The steps are the followings:

- 1) Estimate the unknown AP locations (if known AP location, this can replace the estimated ones). The estimation can be done either via averaging over the positions of few strongest fingerprints (i.e., where that AP was heard with strongest powers) or via using a weighted approach, as the one presented in [14], or by applying a two-step deconvolution process, as described in [5]. Our studies showed that the weighted approach gives slightly better results than the other two, thus it will be selected in our analysis. Since AP location is done in 3D plane, after this step, there will be three parameters to be stored per AP regarding AP position.

2) Associate an underlying path-loss model with the measured RSS and estimate the model parameters via certain statistical methods. In our paper we will discuss two path-loss models: the classical slope-based path-loss model [5] with two additional parameters per AP (transmit power and slope coefficients) and a new simplified path-loss model which focuses on z-dimension only and which has only one parameter. Thus, the number of extracted parameters per AP is 5 or 6, according to the underlying path-loss model.

The **traditional path-loss model** is based on free space wave propagation [15] and involves two modeling parameters per AP: $P_{T_{ap}}$ which is the ap -th AP transmit power and n_{ap} which is the path-loss coefficient of the ap -th AP. Those two parameters are related to the RSS via:

$$P_{i,ap} = P_{T_{ap}} - 10n_{ap}\log_{10}d_{i,ap} + \eta_{i,ap}, \quad (4)$$

where $\eta_{i,ap}$ is a noise factor, typically assumed Gaussian distributed, of zero mean and standard deviation σ . The noise is typically due to shadowing, fading and measurements errors: $\eta_{i,ap} \propto \mathcal{N}(0, \sigma^2)$. Above, $d_{i,ap} = \sqrt{(x_i - x_{ap})^2 + (y_i - y_{ap})^2 + (z_i - z_{ap})^2}$ is the Euclidean distance between the ap -th AP and the i -th measurement point. The above model can be re-written in matrix form as:

$$\mathbf{P}_{ap} = \mathbf{H}_{ap}\boldsymbol{\theta}_{ap} + \mathbf{n} \quad (5)$$

where $\boldsymbol{\theta}_{ap} \triangleq [P_{T_{ap}} \ n_{ap}]^\top$, $\mathbf{P}_{ap} \triangleq [P_{1,ap} \ P_{2,ap} \ \dots \ P_{N_{FP},ap}]^\top$ is the vector with power fingerprints in logarithmic scale coming from ap -th access point, $^\top$ is the transpose operator, \mathbf{n} is a Gaussian distributed $N_{FP} \times 1$ vector with elements $\eta_{i,ap}$ and

$$\mathbf{H}_{ap} \triangleq \begin{bmatrix} 1 & -10\log_{10}d_{1,ap} \\ \dots & \dots \\ 1 & -10\log_{10}d_{N_{FP},ap} \end{bmatrix} \quad (6)$$

2.3. Complexity of model-based approaches versus fingerprinting approach

To address the complexity issue we provide a brief comparison between the complexity of fingerprinting approach and model-based approaches in terms of the memory size required for performing localization in the mobile side. In fingerprinting approach the size of data we need to store in the mobile device is proportional to $N_{fp} \times N_{ap}$ as we need to store all fingerprinting vectors which are of size N_{ap} . However in model-based methods (like the ones proposed in this paper and also in their original non-robust counterparts) the size of data that we need to keep is just proportional to the number of APs, i.e. N_{ap} . For example in the above-mentioned path-loss approach we need to store $5N_{ap}$ parameters, i.e., the 3 coordinates of each AP plus their transmit power and their associated path-loss exponents. In Weighted Centroid Localization [3,14,19,20] approach, we only need to store the 3 coordinates of each AP which means a total of $3N_{ap}$ parameters. This is a significant reduction in the size of data as usually N_{fp} can be a huge number but N_{ap} is limited by the hardware cost employed in the building for internet coverage which is typically tens to hundreds maximum.

3. Robust Floor Estimation Algorithms

In this Section we introduce four robust floor estimation algorithms. We first review the M -estimates of regression which is a method for robust estimation of parameters in a linear regression problem and then based on that robustify four existing indoor localization algorithms for floor estimation.

Consider the linear regression problem

$$\mathbf{y} = \mathbf{H}\mathbf{x} + \boldsymbol{\varepsilon}, \quad (7)$$

Table 2. Functions $\rho(e)$, $\psi(e)$ and $w(e)$ for ordinary least-squares and three commonly-used robust functions.

Method	Objective function $\rho(e)$	Influence function $\psi(e)$	Weight function $w(e)$	95% efficiency tuning constant
LS	$e^2/2$	e	1	none
Huber	$ e \min(e , k) - \frac{1}{2}(\min(e , k))^2$	$\max[-k, \min(k, e)]$	$\min(1, k/ e)$	$k = 1.345$
Bi-square	$\frac{k^2}{6} \left(1 - ((1 - (e/k)^2)_+)^3\right)$	$e((1 - \frac{e^2}{k^2})_+)^2$	$((1 - \frac{e^2}{k^2})_+)^2$	$k = 4.685$
Cauchy	$\frac{k^2}{2} \log(1 + (\frac{e}{k})^2)$	$\frac{e}{(1 + (e/k)^2)}$	$\frac{1}{(1 + (e/k)^2)}$	$k = 2.385$

where \mathbf{H} is the matrix of regressors (for example matrix \mathbf{H}_{ap} in (5)), \mathbf{y} is the $n \times 1$ noisy observation vector, \mathbf{x} denotes the $k \times 1$ parameter vector for which we are going to find an estimate, and $\boldsymbol{\varepsilon}$ denotes the error vector whose entries are assumed to be i.i.d. from a symmetric continuous distribution with an unknown scale parameter s .

Let $e_i = e_i(\mathbf{x}) = y_i - \mathbf{h}_i^\top \mathbf{x}$ denote the i -th residual for a candidate vector \mathbf{x} , where y_i is the i -th entry of \mathbf{y} and \mathbf{h}_i is the i -th row of matrix \mathbf{H} . At this point assume that the scale parameters is known. The ordinary least-squares (LS) tries to minimize $\sum_i e_i^2$, which yields an unstable solution in the presence of outliers or heavy-tailed noise. The M -estimators reduce the effect of outliers and heavy-tailed noise by replacing the sum of squared residuals by the following objective function

$$\sum_{i=1}^n \rho(e_i(\mathbf{x})/s), \quad (8)$$

where $\rho(\cdot)$ is a symmetric, convex, positive-definite function; see, e.g., the upper plot in Figure 1.

Let $\psi = \rho'$ be the derivative of ρ . Then the minimizer of (8) is the solution to the following equation

$$\sum_{i=1}^n \psi(e_i(\mathbf{x})/s) \mathbf{h}_i^\top = 0. \quad (9)$$

Defining $w(e_i) \triangleq \psi(e_i)/e_i$ and denoting $w_i \triangleq w(e_i/s)$, (9) can be re-written as

$$\sum_{i=1}^n e_i(\mathbf{x}) w_i \mathbf{h}_i^\top = 0. \quad (10)$$

Since w_i is itself a function of e_i , to solve (10) we use an iterative algorithm called *iterative re-weighted least squares* (IRLS) [16,17] where in each iteration t an estimate $\hat{\mathbf{x}}_{\{t\}}$ is computed from (10) by assuming that w_i is constant, then the residuals and weights are updated based on $\hat{\mathbf{x}}_{\{t\}}$ which will be used in the next iteration for solving (10) and finding the new estimate $\hat{\mathbf{x}}_{\{t+1\}}$. This iteration continues until a stopping criterion is satisfied. Remark that since the scale s is unknown in practice, it is commonly replaced at each iteration by a robust estimate \hat{s} calculated from the current residuals. A commonly used estimator for scale is the median absolute deviation (MAD) $\hat{s} = \text{MAD}(\mathbf{e}) = 1.4286 \cdot \text{median}_i(|e_i - \text{median}_i(e_i)|)$ which is the default choice in `robustfit` routine of Matlab. From now on, we denote this iterative robust solution to the regression problem of (7) as

$$\text{robustfit}(\mathbf{H}, \mathbf{y}). \quad (11)$$

Choosing the weight function $w(\cdot)$, or equivalently $\psi(\cdot)$ and $\rho(\cdot)$, plays an important role here. In fact the function ρ can be interpreted as $-\log f_e(e/s)$, which means that if the error term has distribution f_e then the IRLS estimate coincides with the maximum likelihood (ML) estimate. In practice, we do not know the error distribution and we choose the weight function so as to alleviate the effect of large errors stemming from impulsive or heavy-tailed noise. This is accomplished

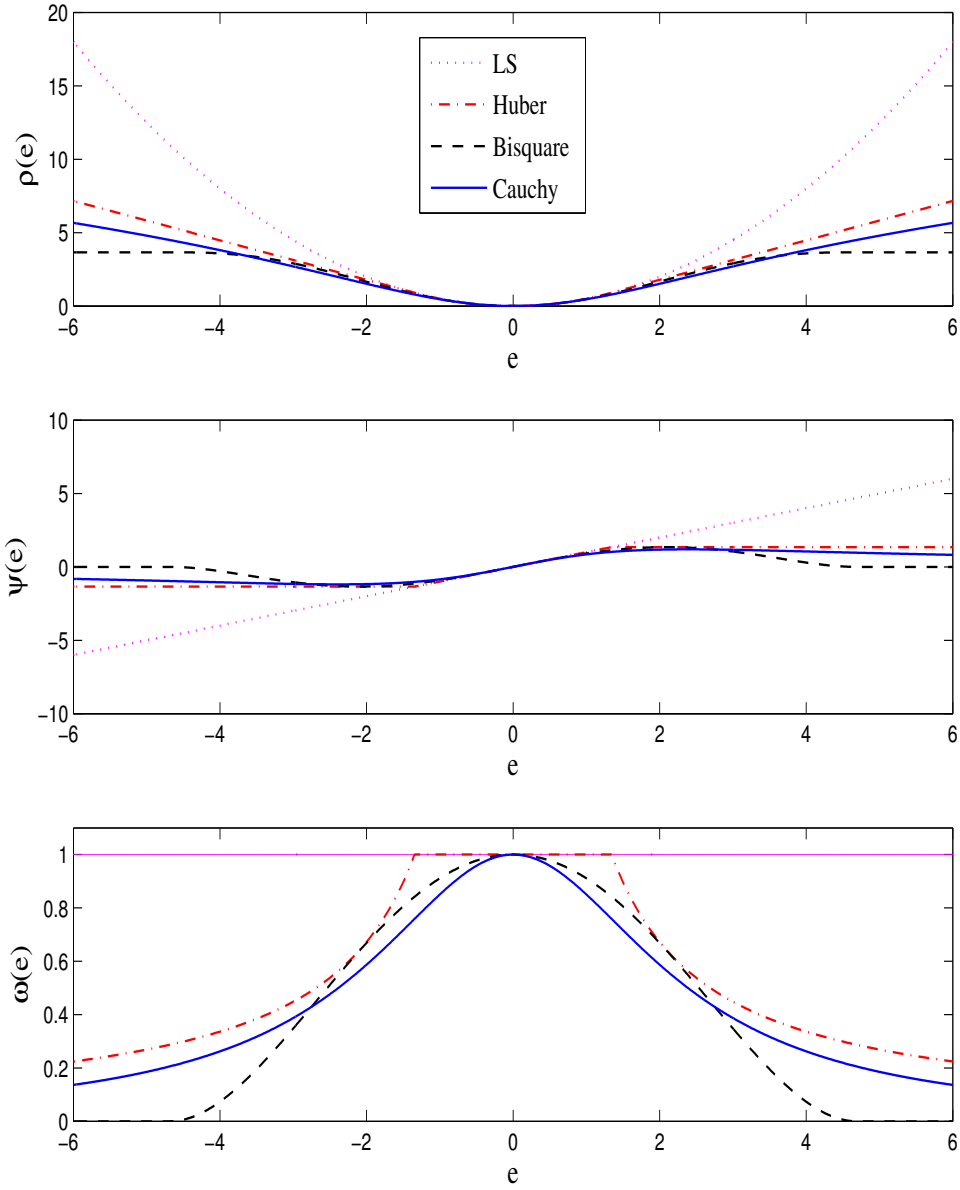


Figure 1. Functions $\rho(e)$, $\psi(e)$, and $w(e)$ for LS and three commonly used robust functions.

191 by choosing bounded $\psi(\cdot)$ functions. Function $\psi(\cdot)$, sometimes called the *influence function* [18],
 192 determines the influence of a datum on the estimate. For example in LS case when $\psi(e) = e$, this
 193 influence is linear which results in the non-robustness of the LS solution. On the other hand by
 194 choosing a bounded ψ , the influence of large errors, stemming from outliers or heavy-tailed noise,
 195 is bounded which results in the robustness of the estimate. Some commonly used robust functions
 196 which will be later used in this paper for robustification of localization approaches are represented in
 197 Table 2 and Figure 1. As it can be seen from Figure 1 all three robust influence functions are bounded.
 198 The constant k is called *tuning constant* which trades between the robustness and the efficiency when
 199 the noise is Gaussian; smaller values of k provide more robustness but are less efficient when the
 200 noise is normally distributed [2].

In what follows we show concrete examples of how these robustification functions can be applied to solve the 3D indoor localization problem.

3.1. Robust Weighted Centroid Localization

Weighted centroid localization (WCL) approach, first proposed for position estimation in wireless sensor networks [3], is a simple and low-complexity but promising localization approach. The position of the MS in the WCL approach is computed as the weighted average of the positions of APs heard by the MS. Denoting the set of all hearable APs by \mathcal{H} and the (known) coordinates of APs by $\mathbf{c}_{ap} \triangleq (x_{ap}, y_{ap}, z_{ap})$, $ap = 1, \dots, |\mathcal{H}|$, the WCL-based estimate of mobile station coordinates is computed as

$$\hat{\mathbf{c}}_{\text{WCL}} = \frac{\sum_{ap \in \mathcal{H}} w_{ap} \mathbf{c}_{ap}}{\sum_{ap \in \mathcal{H}} w_{ap}}, \quad (12)$$

where w_{ap} are weight functions. To weight shorter distances (nearer APs) more than higher distances, w_{ap} may be chosen as [3]

$$w_{ap} = 1/(d_{ap})^g, \quad (13)$$

where d_{ap} is the distance between ap -th AP and the MS, and degree g is to ensure that remote APs still impact the position estimation [3].

Since d_{ap} are not readily available, and also since RSS heard from AP ap is inversely proportional to d_{ap} , the weights w_{ap} in (12) can be replaced by RSS to obtain the following RSS-based formula for WCL [14,19,20]

$$\hat{\mathbf{c}}_{\text{WCL}} = \frac{\sum_{ap \in \mathcal{H}} p_{ap} \mathbf{c}_{ap}}{\sum_{ap \in \mathcal{H}} p_{ap}}, \quad (14)$$

where p_{ap} is the measured RSS of AP number ap .

Equation (14) can be written independently for each coordinate. For instance, for the height coordinate (which is the coordinate that matters in floor detection task) we have

$$\hat{z}_{\text{WCL}} = \frac{\sum_{ap \in \mathcal{H}} p_{ap} z_{ap}}{\sum_{ap \in \mathcal{H}} p_{ap}}, \quad (15)$$

To robustify the WCL approach, we first remark that (15) can be written as

$$\hat{z}_{\text{WCL}} = \arg \min_z \sum_{ap \in \mathcal{H}} |e_{ap}(z)|^2, \quad (16)$$

where $e_{ap}(z) \triangleq \sqrt{p_{ap}}(z - z_{ap})$.

The robust WCL is then obtained by replacing $|e_{ap}(z)|^2$ in the right-hand side of (16) by the general cost function $\rho(e_{ap}(z)/s)$, which yields

$$\hat{z}_{\text{RWCL}} = \arg \min_z \sum_{ap \in \mathcal{H}} \rho\left(\frac{e_{ap}(z)}{s}\right), \quad (17)$$

where s is the scale parameter which can be estimated as discussed in the previous section.

3.1.1. Implications of weighted centroid localization approach

Before proceeding with the next section, we investigate some implications arising from the WCL approach, which will ease the understanding of our assumptions in the next section. We first remark that (16), and hence (15), is the maximum likelihood solution of the following set of $|\mathcal{H}|$ equations

$$\sqrt{p_{ap}} z_{ap} = \sqrt{p_{ap}} z + q_{ap}, \quad \forall ap \in \mathcal{H}, \quad (18)$$

for finding z , where q_{ap} is a zero-mean Gaussian random variable with identical variance for all $ap \in \mathcal{H}$. Equation (18) in fact implies that, according to the WCL approach, the relationship between the received power p_{ap} and the vertical distance between the MS and ap -th access point, $d_{z,ap} \triangleq |z - z_{ap}|$, complies with the following formula

$$d_{z,ap} = \sqrt{\frac{|q_{ap}|^2}{p_{ap}}}. \quad (19)$$

Now, it is easy to verify that the linear scale equation (19) will coincide with the noise-free logarithmic scale path loss model of (4) if

1. Path loss exponent in (4) has the value $n_{ap} = 2$, $\forall ap \in \mathcal{H}$, which is the typical pathloss exponent of free space.
2. $P_{i,ap}$ in (4) relates to p_{ap} as $P_{i,ap} = 10 \log p_{ap}$.
3. $P_{T,ap}$ in (4) relates to random variable q_{ap} as $P_{T,ap} = 10 \log |q_{ap}|^2$. This means that $|q_{ap}|^2$ represents the transmit power of the ap -th AP that is considered as a nuisance parameter here, whose value is not of interest.
4. The distance $d_{i,ap}$ in (4) represents the distance along z -coordinate.

In other words, WCL model (14) can be regarded as a coarse approximation of path-loss model (4) when the four above assumptions are adopted. In fact a beauty of the WCL approach is that despite apparent simplicity and being a coarse approximation of the channel model, which makes it appealing for employing in mobile computing devices, it works very promising.

3.2. Robust Nonlinear Joint Parameter Estimation and Trilateration

Let us denote the location of MS by (x, y, z) . Taking into account the discussion from the previous section, we now start from the assumption that the vertical distance between MS and each AP is proportional to the inverse of square-root of received power, which is

$$|z - z_{ap}| = \frac{c}{\sqrt{p_{ap}}}, \quad ap = 1, 2, \dots, N_{ap}. \quad (20)$$

This model is in line with the observation made in the previous section and equation (19), where $c = |q_{ap}|$ is assumed to be the square root of the identical transmit power of APs.

The task is then to estimate c and z by minimizing the following function

$$F(z, c) = \sum_{ap=1}^{N_{ap}} f_{ap}(z, c)^2, \quad (21)$$

where

$$f_{ap}(z, c) = (|z - z_{ap}| - \frac{c}{\sqrt{p_{ap}}}) \quad (22)$$

Employing the Gauss-Newton method, we obtain the following iterative formula for finding the minimizer of (21)

$$\hat{\theta}_{\{k+1\}} = \hat{\theta}_{\{k\}} - (\mathbf{J}_{\{k\}}^T \mathbf{J}_{\{k\}})^{-1} \mathbf{J}_{\{k\}}^T \mathbf{f}_{\{k\}}, \quad (23)$$

where subscription $\{k\}$ denotes the value in k -th iteration, $\theta \triangleq [z, c]^T$, and

$$\mathbf{J} \triangleq \begin{bmatrix} \frac{\partial f_1}{\partial z} & \frac{\partial f_1}{\partial c} \\ \frac{\partial f_2}{\partial z} & \frac{\partial f_2}{\partial c} \\ \vdots & \vdots \\ \frac{\partial f_{N_{ap}}}{\partial z} & \frac{\partial f_{N_{ap}}}{\partial c} \end{bmatrix}, \quad (24)$$

227 with $\frac{\partial f_{ap}}{\partial z} = \text{sign}(z - z_{ap})$, $\frac{\partial f_{ap}}{\partial c} = \frac{-1}{\sqrt{p_{ap}}}$, and

$$\mathbf{f} = [f_1, f_2, \dots, f_{N_{ap}}]^T. \quad (25)$$

To robustify this algorithm, we notice that the second term in the right hand side of (23) can be interpreted as the LS solution to the regression equation

$$\mathbf{f} = \mathbf{J}\Delta\theta + \text{noise}, \quad (26)$$

for finding $\Delta\theta$. Therefore to robustify (23), we can simply replace this term by IRLS solution of (26) to get the following formula for robust joint estimation of z and c :

$$\hat{\theta}_{\{k+1\}} = \hat{\theta}_{\{k\}} - \text{robustfit}(\mathbf{J}_{\{k\}}, \mathbf{f}_{\{k\}}). \quad (27)$$

228 The method can be easily extended to trilateration case where all the three coordinates (x, y, z) are
 229 assumed to affect the received RSS. Although a more realistic assumption, it deteriorates the floor
 230 detection results in practice, because of entering the errors along nuisance directions x and y to the
 231 problem.

232 3.3. Robust Linear Joint Parameter Estimation and Multilateraion

233 Let us denote the location of MS by (x, y, z) , the coordinates of the i -th AP by (x_i, y_i, z_i) , the
 234 distance of MS to i -th AP by r_i , and the distance between i -th and j -th APs by d_{ij} . Then it can be easily
 235 verified that the set of the following $N_{ap} - 1$ equations are satisfied [4, Section 5].

$$\begin{cases} (x - x_1)(x_2 - x_1) + (y - y_1)(y_2 - y_1) + (z - z_1)(z_2 - z_1) & = 0.5(r_1^2 - r_2^2 + d_{21}^2) \\ (x - x_1)(x_3 - x_1) + (y - y_1)(y_3 - y_1) + (z - z_1)(z_3 - z_1) & = 0.5(r_1^2 - r_3^2 + d_{31}^2) \\ \vdots & \\ (x - x_1)(x_{N_{ap}} - x_1) + (y - y_1)(y_{N_{ap}} - y_1) + (z - z_1)(z_{N_{ap}} - z_1) & = 0.5(r_1^2 - r_{N_{ap}}^2 + d_{N_{ap}1}^2) \end{cases} \quad (28)$$

Assuming that $r_i = \frac{c}{\sqrt{p_i}}$, $i = 1, \dots, N_{ap}$ this can be rewritten in matrix form as

$$\mathbf{G}\mathbf{x} = \mathbf{d}, \quad (29)$$

236 where

$$\mathbf{G} \triangleq \begin{bmatrix} x_2 - x_1 & y_2 - y_1 & z_2 - z_1 & \frac{1}{2}(\frac{1}{p_2} - \frac{1}{p_1}) \\ x_3 - x_1 & y_3 - y_1 & z_3 - z_1 & \frac{1}{2}(\frac{1}{p_3} - \frac{1}{p_1}) \\ \vdots & \vdots & \vdots & \vdots \\ x_{N_{ap}} - x_1 & y_{N_{ap}} - y_1 & z_{N_{ap}} - z_1 & \frac{1}{2}(\frac{1}{p_{N_{ap}}} - \frac{1}{p_1}) \end{bmatrix}, \quad (30)$$

$$\mathbf{x} = [x - x_1, y - y_1, z - z_1, c^2]^T, \quad (31)$$

237 and

$$\mathbf{d} = \frac{1}{2}[d_{21}^2, d_{31}^2, \dots, d_{N_{ap}1}^2]^T. \quad (32)$$

Then the LS solution for joint location estimation and parameter estimation will be

$$\hat{\mathbf{x}} = (\mathbf{G}^T \mathbf{G})^{-1} \mathbf{G}^T \mathbf{d}. \quad (33)$$

Now the robust linear trilateration approach can be obtained by replacing the LS solution by IRLS solution:

$$\hat{\mathbf{x}} = \text{robustfit}(\mathbf{G}, \mathbf{d}). \quad (34)$$

The above robust method can be simplified for estimating the vertical position by removing the first two columns of \mathbf{G} as well as the first two rows of \mathbf{x} and then solving the robust estimation problem in (34).

3.4. Robust Deconvolution-Based Pathloss Estimator

In this part we robustify the deconvolution-based pathloss parameter estimator [5] by employing the IRLS estimator [16,17]. The deconvolution-based approach consists of two main stages: an offline stage during which we estimate the AP parameters and an online stage in which we estimate the MS position. We robustify the algorithm by replacing the ordinary LS approach employed in the offline stage (see [5, Section III]) by the IRLS estimator described earlier.

$$\hat{\Theta}_{i,ap,\text{robust}} = \text{robustfit}(\mathbf{H}_i, \mathbf{P}_{ap}), \quad (35)$$

where \mathbf{H}_i is the matrix built from the AP parameters as in [5, equation (11)] and $\mathbf{P}_{ap} \triangleq [P_{1,ap}, P_{2,ap}, \dots, P_{N_f,ap}]^T$ is the vector whose n -th entry $P_{n,ap}$ is the received power of access point ap at fingerprint n .

4. Measurement-based results

In this section we study the performance of the proposed algorithms through some real-life numerical examples.

4.1. Measurement set-up

The experimental testbed is set-up in four different buildings in our city: University Building 1 (UBldg1) which is a four-storey building inside the university campus, University Building 2 (UBldg2) which is a three-storey building inside the university campus, a six-storey Mall, and a Shopping center (ShCtr) which is a three-storey building. The RSS data collection in each building is accomplished along several tracks (each including tens to hundreds measurement points) and the probability of floor detection results are computed by averaging the results over all tracks in each building.

Table 3 shows the number of floors per building, the number of fingerprints per floor in each building, the total number of fingerprints in each building, the number of APs in each building, the number of test points per floor in each building, and the total number of test points in each building.

Table 3. Description of the measurement buildings

Building	No. of floors	No. of fingerprints/floor	Total No. of fingerprints	No. of APs	No. of test points/floor	Total No. of test points
UBldg1	4	[205, 160, 62, 44]	471	309	[109, 157, 106, 118]	490
UBldg2	3	[113, 162, 107]	382	354	[62, 77, 37]	176
Mall	6	[62, 305, 305, 73, 20, 0]	765	326	[24, 67, 48, 66, 0, 0]	205
ShCtr	3	[28, 169, 16]	213	69	[0, 203, 12]	215

The device employed for collecting the data is an Acer windows tablet with a proprietary software to collect the RSS data which is pictured in Figure 2. The software records the RSS as well as the coordinates by pressing the location point in the building map. The measurement points in the first floor of UBldg1 has been shown in Figure 3. To give an idea of the building structure, a picture taken from the second floor of UBldg1 has been demonstrated in Figure 4.

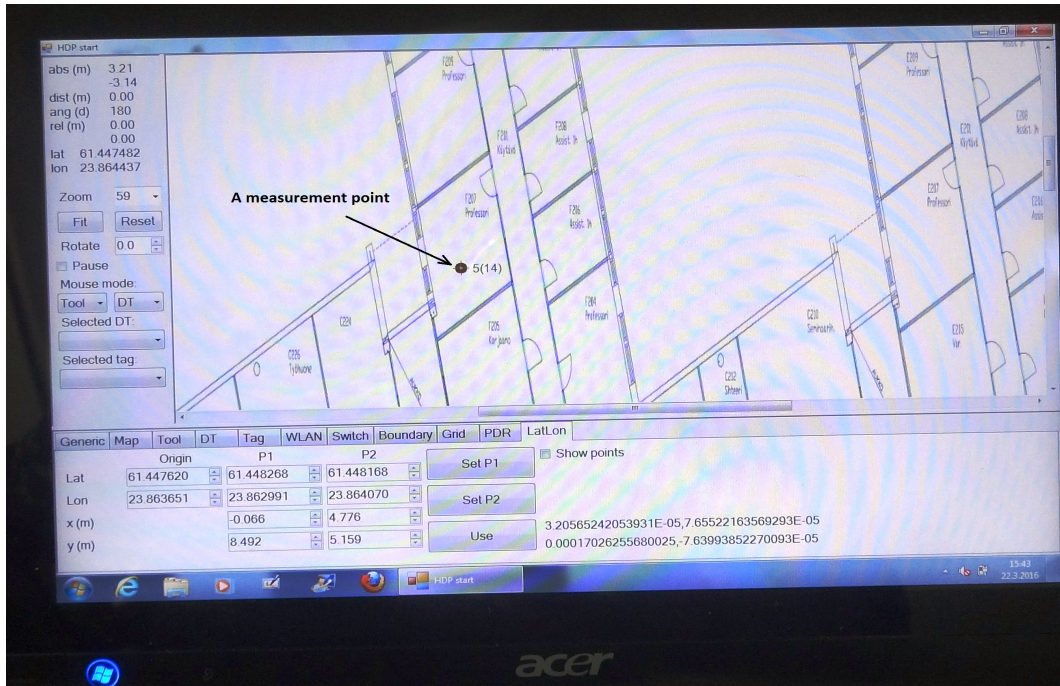


Figure 2. The Acer windows tablet used for collecting data with a sample measurement point shown here. The number outside the parentheses (here, 5) is the fingerprint index and the number inside (here 14) shows the number of access points heard in this point.

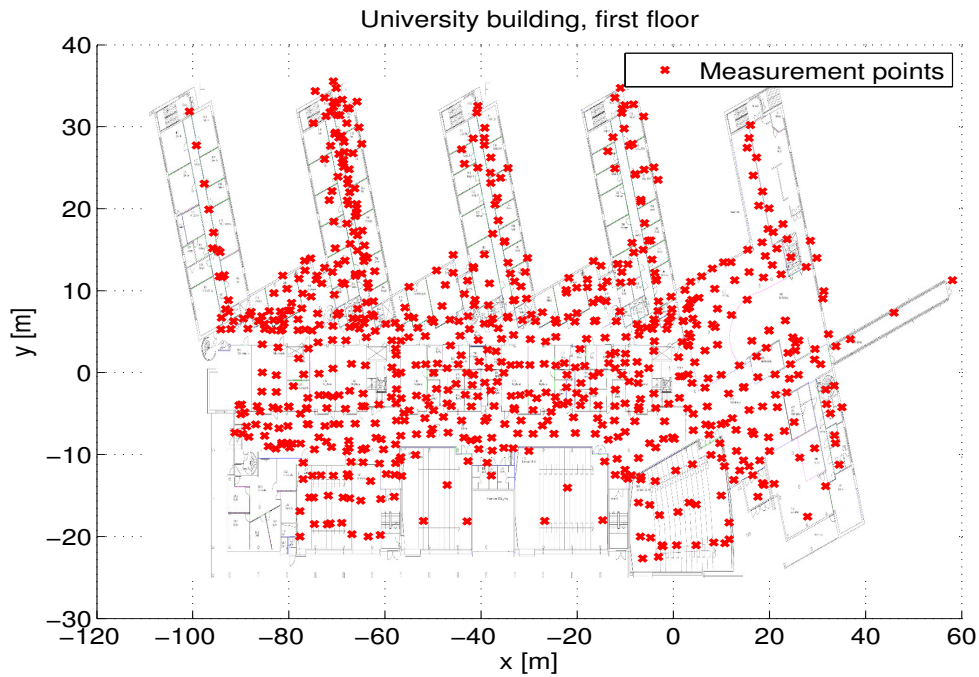


Figure 3. Measurement points in the first floor of UBldg1.

264 4.2. Numerical Results

265 The following three examples study the performance of the robust weighted centroid approach,
 266 robust deconvolution-based approach, and robust nonlinear trilateration approach, respectively.



Figure 4. A picture taken from the second floor of Ubldg1.

Example 1, Robust weighted centroid localization with real data: The first example studies the performance of ordinary WCL and robust WCL approaches with four different robust methods: Huber with parameter $k = 1.345$ (Hub1), Huber with parameter $k = 0.9$ (Hub2), Bi-square with parameter $k = 4.685$ (Bsqr), and Cauchy with parameter $k = 2.385$ (Cau). The results are shown in Table 4. As it can be observed the robust approaches show improvement over the ordinary WCL approach, regardless of the chosen weighting function.

Example 2, Robust deconvolution-based approach with real data: The second example studies the performance of robust deconvolution-based approach compared to the other deconvolution-based approaches when the estimator employed for parameter vector estimation is least-squares (LS), minimum mean-squared error (MMSE), or weighted least-squares (WLS). The robust function used here is Hub1. The data used here is the same as the previous example. The results are shown in Table 5.

As it can be observed the robust approach outperforms the other deconvolution-based approaches for three buildings. The only building in which robust approach is inferior to the others is the Mall in which all detection methods have rather low detection probabilities.

Example 3, Robust nonlinear trilateration with real data: The goal of the third experiment is to study the nonlinear trilateration approach. The data used here is the same as the previous examples. The deconvolution-based approach has been used for estimation of AP positions (we only use the z-coordinate). We employed the ordinary nonlinear trilateration approach [4] as well as its robust version that we introduced here. The results are shown in Table 6. Again the results shows that the robustification has improved the performance. Furthermore, comparison between the second and third columns of the table illustrates how the tuning coefficient affects the performance of the estimator for a given robust weight function. As it can be seen decreasing the value of tuning coefficient implies more robustification.

Concluding Remarks of the experimental tests: The results of the three real-life experiments studied in this section demonstrates the ability of the robust methods to improve the performance of localization algorithms used for floor detection in indoor environments. For instance, comparing Hub1 with the ordinary methods in Tables 4, 5, and 6 shows improvement everywhere other than

Table 4. Comparison of the floor detection probability for different WCL approaches. Column 2 shows the basic approach, columns 3 to 6 are the robust WCL approach with various robust functions: Hub1 (Huber with tuning coefficient $k = 1.345$), Hub2 (Huber with tuning coefficient $k = 0.9$), Bsq (Bi-square with tuning coefficient $k = 4.685$), and Cau (Cauchy with $k = 2.385$). The highest probability in each row has been shown in Bold. All of the robust methods outperform the ordinary WCL.

Building	WCL	RWCL with Hub1	RWCL with Hub2	RWCL with Bsq	RWCL with Cau
UBldg1	0.852	0.858	0.866	0.860	0.860
UBldg2	0.904	0.904	0.902	0.899	0.904
Mall	0.815	0.839	0.836	0.839	0.839
ShCtr	0.827	0.827	0.827	0.827	0.827
Total	0.850	0.857	0.858	0.856	0.858

Table 5. Comparison of the floor detection probability for different deconvolution-based approaches. Column 2-4 show the basic deconvolution approaches as introduced in [5], last column shows the robust deconvolution approach. The robust method outperforms all of the basic deconvolution approaches.

Building	Deconv. LS	Deconv. MMSE	Deconv. WLS	Robust Deconv. with Hub1
UBldg1	0.769	0.771	0.768	0.818
UBldg2	0.899	0.907	0.894	0.925
Mall	0.448	0.473	0.455	0.434
ShCtr	0.649	0.649	0.649	0.667
Total	0.665	0.677	0.666	0.683

Table 6. Comparison of the floor detection probabilities for nonlinear trilateration approach (NTL) and four robust NTL (RNTL) versions of it. All of the robust methods outperform the ordinary nonlinear trilateration.

Building	NTL	RNTL with Hub1	RNTL with Hub2	RNTL with Bsq	RNTL with Cau
UBldg1	0.785	0.790	0.821	0.816	0.813
UBldg2	0.685	0.698	0.725	0.691	0.695
Mall	0.665	0.697	0.687	0.700	0.700
ShCtr	0.796	0.796	0.792	0.792	0.796
Total	0.733	0.745	0.756	0.750	0.751

the Mall building for deconvolution-based method. This is because the Mall building studied in this experiment has a very spacious middle area and therefore can better comply with the Gaussianity assumption in path loss model which is the core of deconvolution-based algorithm.

5. Simulation Example

In this section we study the performance of the proposed robust linear trilateration approach compared to the ordinary linear trilateration [4] through a simulation example. Remark that for evaluating this method we use simulation instead of real data because the linear trilateration is very sensitive to the coordinates of the AP which is chosen as the reference point due to the fact that all the distances are determined with respect to this reference point (see, e.g., (28) and (30) where all distances are with respect to AP number 1). In the real data used for the first three experiments we do not have the exact coordinate of any of the APs to choose it as the reference point. Therefore the linear

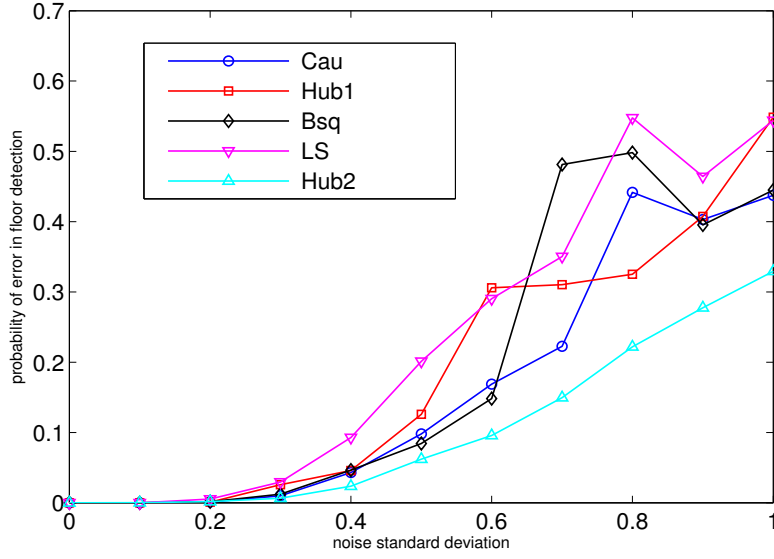


Figure 5. The performance of linear trilateration approaches for different robust weight functions.

trilateration methods are here examined through a simulation example in which the exact location of APs is assumed known. The number of access points with known locations in the simulation is $N_{ap} = 80$ which are located in a 4-storey building with 20 APs in each floor. The area of each floor is $50m \times 50m$ and the floor height is $4m$. All the APs have the same transmit power and the path loss exponent is set to $n_{ap} = 2$, $\forall ap$. The receiver noise variance varies from 0 to 1. The number of random runs (the random location of MS in the building) is 10^5 . The floor detection is performed by first estimating the 3-D coordinates of the MS as in (34) and then rounding the estimated z-coordinate to the height of nearest floor. As it can be seen the robust methods surpass the ordinary LS method. The best performance belongs to the Hub2, Huber robust function with tuning constant $k = 0.9$, which provides more robustness compared to the case $k = 1.345$.

6. Conclusion

In this paper we proposed four robustification methods for floor detection on mobile devices. This was accomplished by exploiting the M-estimators to robustify four existing probabilistic positioning approach with the goal of applying them to the problem of floor detection from RSS measurements in the indoor environment. The first approach was obtained by robustifying the weighted centroid localization approach by replacing the ordinary sum of squared errors by a more general cost function. The second and third approaches were, respectively, a linear and a nonlinear trilateration approaches that first adopt a simplified path loss model and then estimate the position of MS using robust regression methods. The methods need the information of AP locations as a prerequisite. We finally robustified the deconvolution-based approach [5] via replacing the ordinary least-squares estimator by an iterative reweighted least-squares estimator.

The performance of the proposed robust schemes were exemplified both via real-life measurements (Examples 1 to 3 in Section 4.2) and simulations (Figure 5) and all of the proposed robust methods were compared with their non-robust counterparts. In addition, such robust schemes can find their applicability in many LBS applications, such as in the emergency application (e.g., the fast identification of the damaged floors in case of floods or fire), in advertising (e.g., fast finding of the nearby shops at the user's floor with the desired items), etc. Also, the proposed robustification results can be used jointly with additional sensors, such as barometers, when available on the user mobile for an increased positioning accuracy.

The main findings of our paper is that, by using robustification, we can achieve better results than without robustification. The proposed mobile-computing based floor detection algorithms, which use the heard RSS information from APs, are indeed feasible with today's existing WLAN infrastructures.

Bibliography

1. Zhang, N.; Feng, J. *Polaris : A Fingerprint-Based Localization System over Wireless Networks*. Book Chapter, Lecture Notes in Computer Science, Springer, 2012.
2. Fox, J. Robust regression. Appendix to An R and S-Plus Companion to Applied Regression, 2002.
3. Blumenthal, J.; Grossmann, R.; Golatowski, F.; Timmermann, D. Weighted centroid localization in zigbee-based sensor networks. *Intelligent Signal Processing*, 2007. WISP 2007. IEEE International Symposium on. IEEE, 2007, pp. 1–6.
4. Hereman, W.; Murphy, W.S.J. Determination of a position in three dimensions using trilateration and approximate distances. *MCS-95-07* **1995**.
5. Shrestha, S.; Talvitie, J.; Lohan, E.S. Deconvolution-based indoor localization with WLAN signals and unknown access point locations. *International Conference on Localization and GNSS (ICL-GNSS 2013)*; , 2013.
6. Razavi, A.; Valkama, M.; Lohan, E.S. K-Means Fingerprint Clustering for Low-Complexity Floor Estimation in Indoor Mobile Localization. *2015 IEEE Globecom Workshops (GC Wkshps)*, 2015.
7. Xia, H.; Wang, X.; Qiao, Y.; Jian, J.; Chang, Y. Using multiple barometers to detect the floor location of smart phones with built-in barometric sensors for indoor positioning. *Sensors* **2015**, *15*, 7857–7877.
8. Rahman, A.; Amiruddin, M.; Dashti, M.; Zhang, J. Floor determination for positioning in multi-story building. *Wireless Communications and Networking Conference (WCNC)*, 2014 IEEE. IEEE, 2014, pp. 2540–2545.
9. Bahl, P.; Padmanabhan, V.N. RADAR: An in-building RF-based user location and tracking system. *INFOCOM 2000. Nineteenth Annual Joint Conference of the IEEE Computer and Communications Societies. Proceedings. IEEE. Ieee*, 2000, Vol. 2, pp. 775–784.
10. Roos, T.; Myllymäki, P.; Tirri, H.; Misikangas, P.; Sievänen, J. A probabilistic approach to WLAN user location estimation. *International Journal of Wireless Information Networks* **2002**, *9*, 155–164.
11. Kuo, S.P.; Wu, B.J.; Peng, W.C.; Tseng, Y.C. Cluster-enhanced techniques for pattern-matching localization systems. *Mobile Adhoc and Sensor Systems*, 2007. MASS 2007. IEEE International Conference on. IEEE, 2007, pp. 1–9.
12. Duda, R.O.; Hart, P.E.; others. *Pattern classification and scene analysis*; Vol. 3, Wiley New York, 1973.
13. Liu, H.; Darabi, H.; Banerjee, P.; Liu, J. Survey of wireless indoor positioning techniques and systems. *Systems, Man, and Cybernetics, Part C: Applications and Reviews, IEEE Transactions on* **2007**, *37*, 1067–1080.
14. Murray, J.; Tarlow, B. Wi-Fi position fix. European patent application EP 2574954A1, 2013.
15. Nurminen, H.; Talvitie, J.; Ali-Loytty, S.; Müller, P.; Lohan, E.S.; Piche, R.; Renfors, M. Statistical Path Loss Parameter Estimation and Positioning Using RSS Measurements in Indoor Wireless Networks. In *2012 International Conference on Indoor Positioning and Indoor Navigation (IPIN2012)*, 2012.
16. Huber, P. *Robust Statistics*; Wiley Series in Probability and Statistics, John Wiley & Sons, 2004.
17. Maronna, R.; Martin, R.; Yohai, V. *Robust Statistics: Theory and Methods*; Wiley Series in Probability and Statistics, Wiley, 2006.
18. Zhang, Z. Parameter estimation techniques: A tutorial with application to conic fitting. *Image and vision Computing* **1997**, *15*, 59–76.
19. Wang, J.; Urriza, P.; Han, Y.; Cabric, D. Weighted centroid localization algorithm: theoretical analysis and distributed implementation. *Wireless Communications, IEEE Transactions on* **2011**, *10*, 3403–3413.
20. Liu, Y.; Yi, X.; He, Y. A novel centroid localization for wireless sensor networks. *International Journal of Distributed Sensor Networks* **2012**, 2012.

© 2016 by the authors. Submitted to *Sensors* for possible open access publication under the terms and conditions of the Creative Commons Attribution license (<http://creativecommons.org/licenses/by/4.0/>)